

Supporting information for

Fe³⁺-Enhanced NIR-to-NIR upconversion nanocrystals for tumor-targeted trimodal bioimaging

Zhengbin An,^a Lijia Wang,^a Chan Gao,^a Ni He,^a Baode Zhu,^b Yingju Liu^{*,c} and Qingyun Cai^{*,a}

^a State Key Lab of Chemo/Biosensing and Chemometrics, College of Chemistry and Chemical Engineering, Hunan University, Changsha, 410082, China

^b State Key Laboratory of Developmental Biology of Freshwater Fish, The National & Local Joint Engineering Laboratory of Animal Peptide Drug Development, College of Life Sciences, Hunan Normal University, Changsha, 410081, China

^c College of Materials & Energy, South China Agricultural University, Guangzhou 510642, China, liuyingju@hotmail.com

*Corresponding author. E-mail: qycail0002@gmail.com; Fax.: +86-0731-88821848

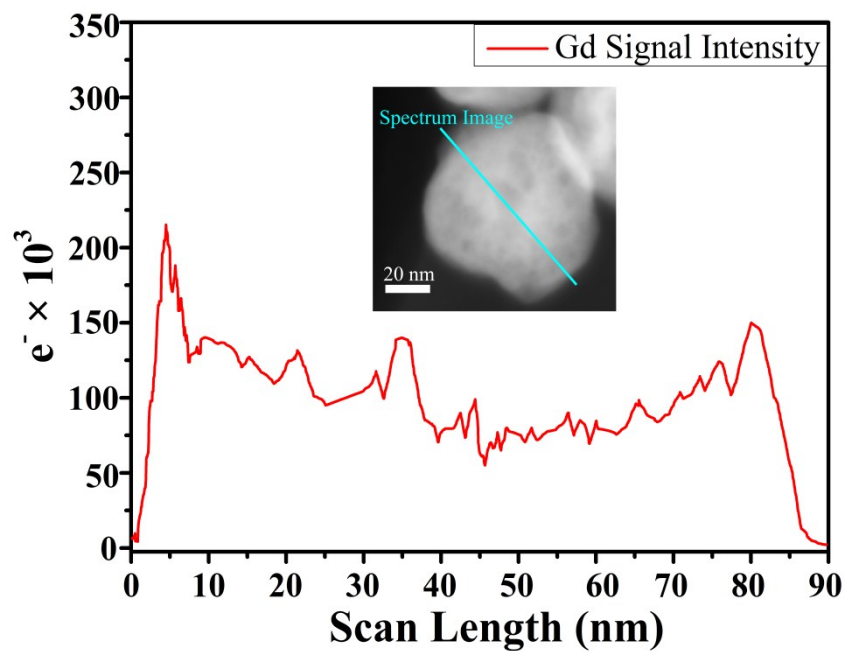


Fig. S1 EELS line scan conducted with HAADF image (inset) on a Y:Yb,Tm,Fe@Gd nanoparticle showing Gd residing predominantly in the shell.

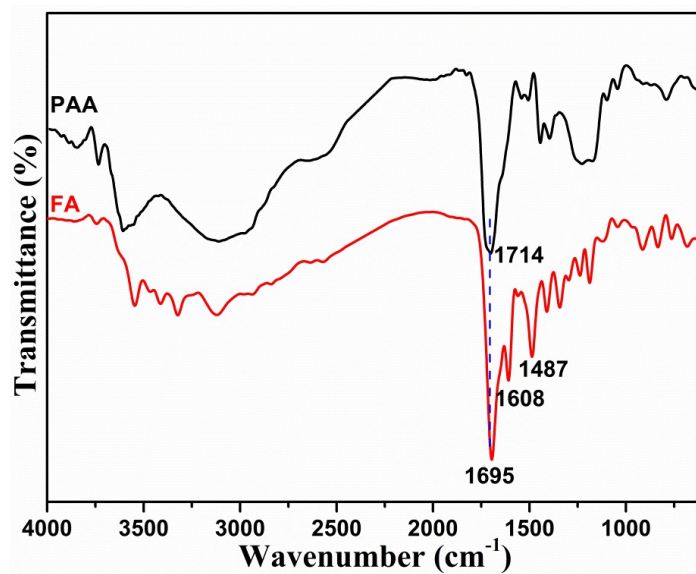


Fig. S2 Fourier transform infrared spectroscopy of PAA and FA.

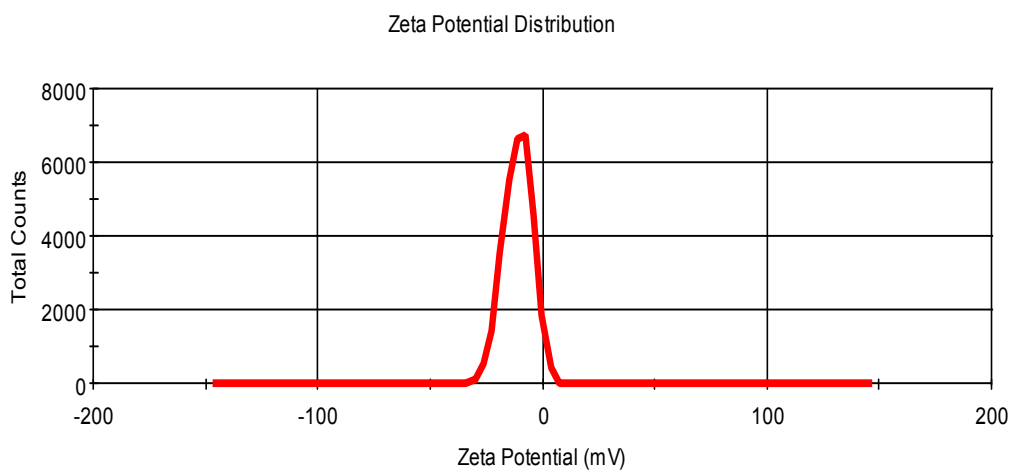


Fig. S3 Zeta potential of FA-Y:Yb,Tm,Fe@Gd NPs.

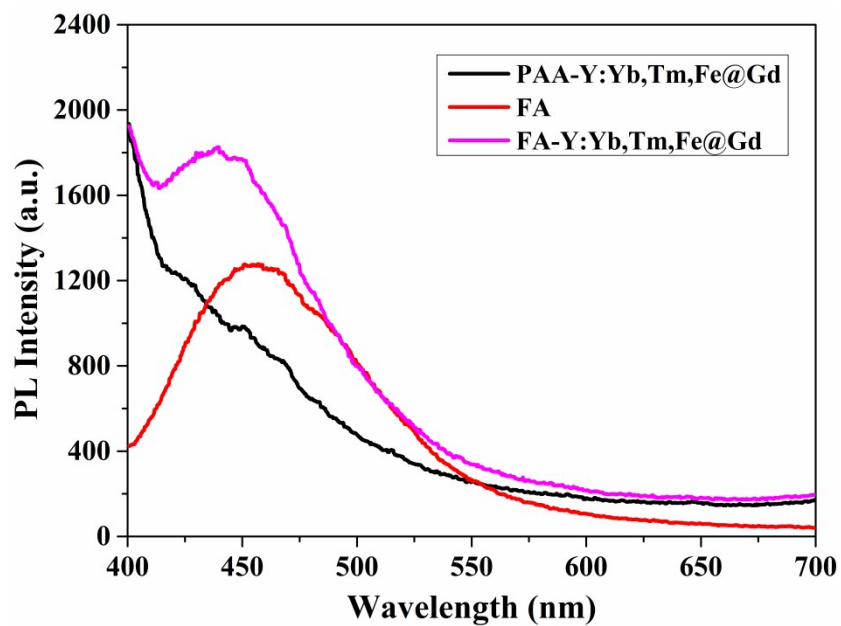


Fig. S4 Comparison of the photoluminescence characteristic spectra before and after FA-modification of PAA-Y:Yb,Tm,Fe@Gd NPs in water excitation at 370 nm.

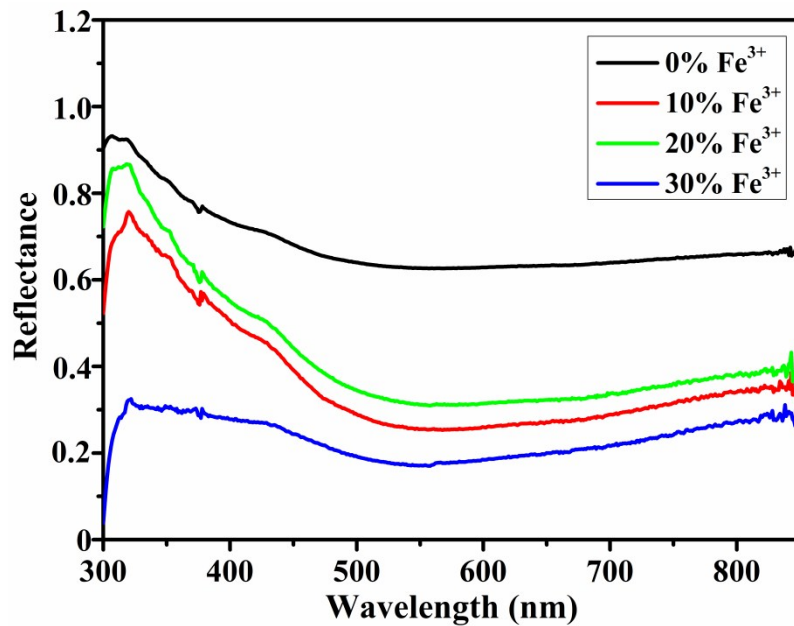


Fig. S5 Diffuse reflectance spectra for Fe^{3+} -free and x mol% Fe^{3+} codoped $\text{NaYF}_4:\text{Yb},\text{Tm}$ ($x=10, 20$ and 30) nanoparticles.

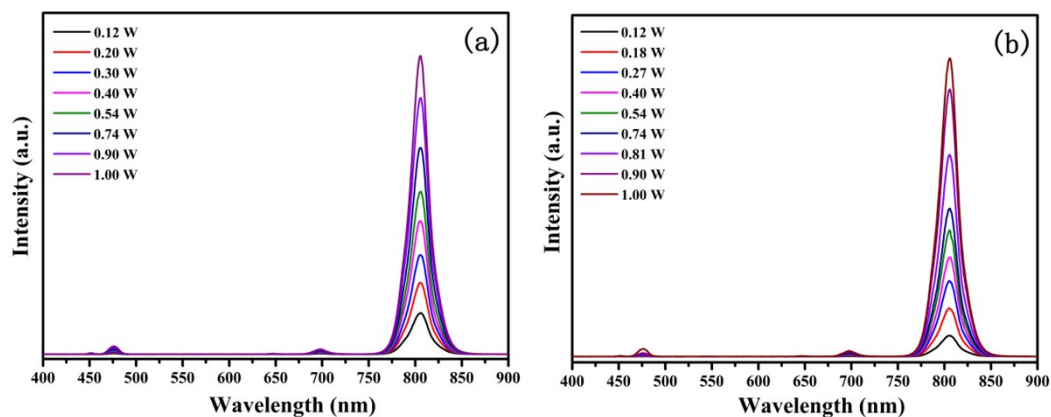


Fig. S6 Upconversion luminescence spectra of (a) cit-Y:Yb,Tm NPs, (b) cit-Y:Yb,Tm,Fe NPs with the different power intensity at 980 nm.

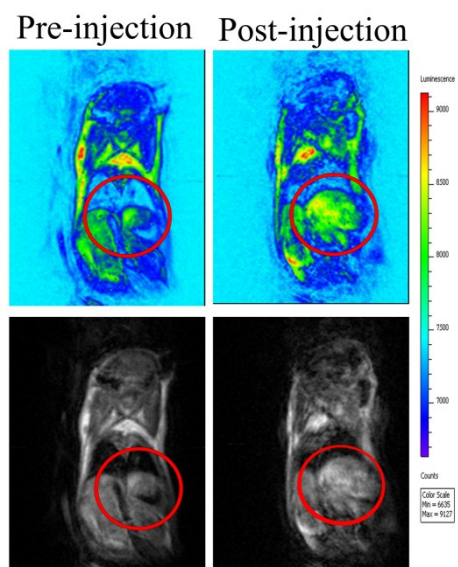


Fig. S7 In vivo MR imaging of Kunming mice after intravenous injection of FA-Y:Yb,Tm,Fe@Gd NPs for 1h.